LAWRENCE
LIVERMORE
NATIONAL
LABORATORY

UCRL-JRNL-227999

# Regional Body-Wave Attenuation Using a Coda Source Normalization Method: Application to MEDNET Records of Earthquakes in Italy

W. R. Walter, K. Mayeda, L. Malagnini, L. Scognamiglio

February 13, 2007

Geophysical Research Letters

# Regional Body-Wave Attenuation Using a Coda Source Normalization Method: Application to MEDNET Records of Earthquakes in Italy

William R. Walter[1], Kevin Mayeda[2], Luca Malagnini[3], and Laura Scognamiglio[3]

[1]Earth Science Division, Lawrence Livermore National Laboratory, Livermore, CA, USA
[2]Weston Geophysical Corporation, Lexington, MA, USA
[3]Istituto Nazionale di Geofisica e Vulcanologia, Rome, Italy

## Abstract

We develop a new methodology to determine apparent attenuation for the regional seismic phases Pn, Pg, Sn, and Lg using coda-derived source spectra. The local-to-regional coda methodology (Mayeda, 1993; Mayeda and Walter, 1996; Mayeda et al., 2003) is a very stable way to obtain source spectra from sparse networks using as few as one station, even if direct waves are clipped. We develop a two-step process to isolate the frequency-dependent $Q$. First, we correct the observed direct wave amplitudes for an assumed geometrical spreading. Next, an apparent $Q$, combining path and site attenuation, is determined from the difference between the spreading-corrected amplitude and the independently determined source spectra derived from the coda methodology. We apply the technique to 50 earthquakes with magnitudes greater than 4.0 in central Italy as recorded by MEDNET broadband stations around the Mediterranean at local-to-regional distances. This is an ideal test region due to its high attenuation, complex propagation, and availability of many moderate sized earthquakes. We find that a power law attenuation of the form $Q(f)=Q_o f^{\gamma}$ fit all the phases quite well over the 0.5 to 8 Hz band. At most stations, the measured apparent $Q$ values are quite repeatable from event to event. Finding the attenuation function in this manner guarantees a close match between inferred source spectra from direct waves and coda techniques. This is important if coda and direct wave amplitudes are to produce consistent seismic results.

## 1. Introduction

The separation of source and path effects is a longstanding problem in seismology. To estimate the portion of path effect due to attenuation ($1/Q$) requires a further division into effects associated with propagation, such as geometrical spreading, scattering, intrinsic attenuation, and site effects. Many standard attenuation analysis methods make assumptions about the source, geometrical spreading, and site effects or else solve for them along with $Q$ and endure the tradeoffs. There are ways to form ratios or averages to cancel out some of these terms, but such approaches usually impose additional restrictions on data or tradeoffs in the results. For this reason, most estimates of $Q$ are tightly coupled to their source, spreading, and site assumptions and/or solutions. Consequently, attenuation estimates that use differing assumptions for these parameters

will not agree with each other. This can limit the utility of published attenuation studies for new applications that may have different source, geometrical spreading, and site effect assumptions. In this study we seek regional direct wave attenuation solutions consistent with results obtained using local-to-regional coda techniques.

Local and regional S-wave coda envelopes have provided some of the most stable and lowest variance estimates of seismic source spectra (e.g., Mayeda, 1993; Mayeda and Walter, 1996; Mayeda et al., 2003; Eken et al., 2004; Morasca et al., 2005; Mayeda et al. 2005). Because the seismic coda consists of scattered energy and is measured over a relatively long time window, it produces amplitude measures that average effects like directivity, radiation pattern, and lateral heterogeneity. In general, coda-derived amplitudes are three-to-five times more stable than those from direct waves such as Sn or Lg. This means that coda-derived source spectra from a single station are equivalent to direct wave results from a 9-to-25 station network. In addition, the coda method can be applied to data with clipped direct wave arrivals, thus allowing the analysis of large magnitude events at local distances.

The availability of independently determined source spectra from coda techniques motivated us to use them to find path corrections for spectra from the regional direct phases Pn, Pg, Sn, and Lg. These results can shed light on the attenuation structure and tectonic evolution of a region, as well as have utility in hazard analysis for predicting ground amplitudes of future damaging earthquakes. Path corrections for regional phases also play an important role in calibrating regional phase earthquake/explosion discriminants such as P/S ratios (e.g., Taylor et al., 2002; Battone et al., 2002 ). Discriminating explosions from earthquakes is important for nuclear test monitoring as well as producing earthquake catalogs free of mining explosions for hazard applications. Finally, these path corrections allow the estimation of source spectra from the regional phases in a manner consistent with those produced using coda techniques.

## 2. Data

The Apennine system of central Italy consists of late Miocene to Pleistocene thrust and fold structures with north-east orientation resulting from the complex relative motion between the Africa and Eurasia plates. The Apennine chain results from the contemporaneous opening of the Tyrrhenian sea, the north-eastward migration of a compressive front, and the flexural retreat of the lithospheric Adria plate dipping below the Italian peninsula (Malinverno and Ryan, 1986; Royden et al., 1987; Patacca et al., 1990; Doglioni et al., 1994). As a consequence of early Miocene compressive front north-eastward migration, the Apennines is characterized by reverse faulting in the front of the chain and extension within the mountain range accommodated by moderate and large normal faulting earthquakes (Pantosti et al., 1996; Montone et al., 1999; Galadini and Galli, 2000; Pondrelli et al., 2002).

We have selected 50 central Italian earthquakes from the time period between 1992-2000 with magnitudes greater than 4.0, which were recorded by MEDNET broadband stations

around the Mediterranean at local-to-regional distances for analysis, as shown in Figure 1. The earthquakes include a number of events from the 1997-1998 Umbria-Marche sequence (e.g., Ekström et al., 1998). An example of observed seismograms from an April, 1998 Mw 5.1 earthquake are shown in Figure 2. In some cases, clear regional phases such as Pn and Sn at station VTS and VSL are observed. In other cases, the regional phases are more complex. We use group velocity windows to define regional phase windows for analysis. Since the source region is relatively small and the events well located, the group velocity windows ensure that for each phase, only energy that has followed a similar path is measured for each event. The data was instrument corrected and rotated to vertical, radial, and transverse components. Regional P-wave measures for Pn and Pg were made on the vertical components and S-wave measures for Sn and Lg on the transverse. Examples of regional phase spectra are shown in Figure 3a.

The coda analysis followed the methodology of Mayeda et al., (2003) and was restricted to data from the local stations AQU and CII that are within 210 km of all events. Log amplitude envelopes of the scattered energy are formed from the two horizontal components after filtering in 11 narrow frequency bands ranging between 0.1 and 8 Hz. At short ranges, the coda amplitude shows little variation with distance making inter-event coda amplitude comparisons using local data particularly robust. We followed the procedure of Mayeda et al., (2003) where interstation scatter of coda amplitudes between the two stations is minimized to get distance corrections. Then, independent waveform modeled moments from Ekstrom et al., (2003) and the INGV Italian CMT catalog (Pondrelli et al, 2006: http://www.ingv.it/seismoglo/RCMT/Italydataset) were used to calibrate the coda spectra in an absolute sense to obtain true source spectra for the 50 events. An example of a coda-derived source spectrum is shown in Figure 3b.

## 3. Apparent Q Procedure

For body waves in media where the velocity is slowly varying, we may use ray theory to write the expression for the P or S-wave far-field displacement (Aki and Richards, 1980, p. 116):

$$u_i(t+T_i) = F_i \dot{M}_o(t) \;\; E_i(R,t) \qquad where \;\; F = \frac{R^i_{\theta\phi}}{4\pi\rho_s^{1/2}\rho_r^{1/2}c_s^{5/2}c_r^{1/2}} \tag{1}$$

where $T_i$ is the ray travel time, $R_{\theta\phi}$ is the point source radiation pattern, $\dot{M}_o(t)$ is the time derivative of the point source moment time function, $\rho$ is the density, $c$ is the wave velocity, $E(R,t)$ is the total path effect which includes geometrical spreading and any attenuation. The subscripts $s$ and $r$ denote source and receiver material properties, respectively. The equation applies to both P and S-waves with appropriate changes to the wave velocity $c$, source radiation pattern, and geometrical spreading. The subscript $i$ indicates the particular P or S phase that we are modeling. This paper is focused on the regional phases, the crustal propagating P and S-waves labeled Pg and Lg respectively and the uppermost mantle propagating P and S-waves labeled Pn and Sn respectively. Here we use source and receiver densities of 2700 and 2500 kg/m$^3$; P-wave source and

receiver velocities of 6 km/s and 5km/s; S-wave source and receiver velocities of 3.5 km/s and 2.9 km/s; and P and S-wave point source radiation pattern terms of 0.44 and 0.60.

It should be noted that it is not necessary to break the total path effect into subcomponents, since these will trade off non-uniquely against each other. One could simply solve for the total path effect and use it to produce source spectra from future direct wave observations. However, it is both commonplace and easier to interpret results if we subdivide the total path effect into a pure geometrical spreading function, a pure apparent attenuation function, and pure site effect function, and therefore we do so here. In the frequency domain, the observed far-field displacement spectra $u_i(f)$ for phase $i$ is then given by:

$$u_i(f) = F_i \dot{M}_o(f)\ G_i(R)\ B_i(R,f) P_i(f) \tag{2}$$

where $f$ is frequency and we have broken the path effect into a pure geometrical spreading term $G(R)$, an apparent attenuation term $B(R, f)$, and a site effect term $P(f)$. We follow Street *et al.* (1975) to define a geometrical spreading factor that has a critical distance $R_o$ within which the spreading is spherical and beyond which it decays as distance to the power $\eta$.

$$G(R) = \begin{cases} \dfrac{1}{R} & \text{where} \quad R < R_o \\ \dfrac{1}{R_o}\left(\dfrac{R_o}{R}\right)^{\eta} & \text{where} \quad R \geq R_o \end{cases} \tag{3}$$

This formulation accounts for the crustal waveguide effect on some phases such as Pg and Lg. We used $\eta$=0.5 at large distances for these phases. For upper mantle phases Pn and Sn we can set $R_o$ to a small number (e.g., 1 m), so the spreading goes as $1/R^{\eta}$ for all distances. These upper mantle phases have larger amplitudes and different frequency content than classical head waves and are more consistent with multiple turning rays traveling in a mantle lid. Following Sereno and Given (1990) we use an exponent slightly greater than one ($\eta$=1.1), consistent with the geometrical effect of Earth curvature for Pn and Sn.

The MEDNET stations are all high quality rock sites located in vaults or tunnels and we expect site effects to be relatively small. We approximate $P(f)$ = 1 and interpret the attenuation as a purely path effect, or to the extent there are significant site effects, this approximation combines that term together with the path attenuation, and solves for a single apparent $Q$. It is important to note that we are not trying to separate intrinsic and scattering attenuation. Rather, for a given geometrical spreading, we model the remaining amplitude effect as an apparent attenuation defined in terms of the Quality or $Q$ factor:

$$B_i(R,f) = e^{-\frac{\pi f R}{Q_i(f) c_i}} \tag{4}$$

$c_i$ is the group velocity of phase $i$ and $Q(f)$ is the frequency dependent quality factor. We can now use these equations to solve for apparent $Q(f)$ by taking the base ten logarithm of equation (2) and substituting in the attenuation function in equation (4) we find:

$$Q_i(f) = \left( \frac{-\pi f R \log e}{c_i} \right) \Big/ \left( \log(u_i(f) - [\log(F_i) + \log(\dot{M}_o(f) + \log(G_i(R)] \right) \tag{5}$$

Given a source moment-rate spectra, here derived from coda, and assuming a geometrical spreading, we can then solve directly for apparent attenuation from the observed instrument-corrected spectra of each regional phase. We illustrate the procedure in Figure 3. The instrument-corrected displacement spectra from the windowed Pn and Sn phases for the April 3, 1998 earthquake recorded at station VTS are shown in black in Figure 3a. We log average and resample the spectra into the same frequency bands used in deriving the coda spectra. Those spectra are shown in color in Figure 3a. The resampled spectra are corrected for geometrical spreading and the far-field Green's function factor $F_i$ from equation (1). These corrected spectra are compared with the coda source spectra in terms of moment-rate in Figure 3b. The difference between the corrected spectra and the source spectra is due to the apparent attenuation. Using equation (5), we solve for the apparent attenuation $Q$ at each frequency. The results are shown in Figure 3c where the Pn and Sn $Q$'s are found to be very similar and show a nearly linear dependence on frequency.

We repeat this process for each earthquake for each phase at each station. We required the ratio of phase signal to pre-event noise to exceed two, otherwise the $Q$ estimate was discarded. The results for all events at station VTS for phases Pn and Sn are shown in Figures 4a and 4b. Each line represents the $Q$ determination from a particular event. Note that the results are fairly stable from event to event, particularly for Sn. We take a log average $Q$ at each frequency and determine a log average standard deviation at each frequency, as shown in Figures 4c and 4d.

Given the approximately linear nature of the observed $Q$ values with frequency, we fit the average values using a simple frequency-dependent power law:

$$Q(f) = Q_o f^{\gamma} \tag{6}$$

The average power law $Q$ values and uncertainties for each station and phase are given in Table 1. Applying the average power law $Q$ to the spectra in Figure 3b we see in Figure 3d that we can match the coda derived source spectra to the level of the inherent scatter of direct wave spectra. Thus, the apparent $Q$ values in Table 1 can be used along with the assumed geometrical spreading to estimate source spectra from the direct regional phases for future central Italian earthquakes.

Next, we applied this process to all six stations. Most of the events at stations AQU and CII were within the Pn-Pg cross over, so only Pg and Lg were measured. In the case of AQU, we imposed a minimum distance of 50 km because at closer distances the limited attenuation combined with the inherent scatter of the amplitude spectra made the measurements less stable, with occasional infinite $Q$ values. Stations VSL and VTS did not show evidence of significant Pg and Lg energy above the Pn and Sn coda levels and so those amplitudes were not calculated.

## 4. Discussion

The resulting apparent attenuation values in Table 1 appear to be consistent with the lithospheric structure in the region and the limited prior regional phase attenuation work. The two local distance stations AQU and CII have paths primarily in the central Apennines and show very strong attenuation, consistent with previous work (e.g. Malagnini et al. 2000a,b). For example, Bindi et al., (2004) using different stations, a closer distance range (5-40 km), different geometrical spreading assumption ($R^{-0.9}$) and different source assumptions, obtained an S-wave $Q(f) = 49f^{0.9}$ for 0.5 to 8 Hz from the 1997-1998 Umbria-Marche events. While the eastern and western Alps are somewhat less attenuating (e.g. Malagnini et al, 2002; Morasca et al. 2006), the events recorded at stations TRI and BNI have significant portions of their paths in the Apennines and the Po river sedimentary basin producing low $Q$ values as well.

Regional wave propagation characteristics beyond the Italian peninsula have been mainly qualitative (e.g. Mele et al. 1997). The regional paths to station VSL pass beneath the oceanic Tyrrhenian Sea where Pg and Lg do not efficiently propagate; however, Pn and Sn are visible to high frequencies. The relatively low $Q$ value for Sn in the upper mantle is consistent with high heat flow and the continued opening of the sea floor. The paths to VTS are mainly within the relatively stable Adria plate and have the highest $Q$ of the 6 paths studied here.

The application of the coda source normalization method shown here was for clusters of events with common paths to each station, but the same procedure could be applied to each event-station pair without the averaging and power law fitting steps. This would provide a path-specific apparent $Q$ that could be used in a 2-D $Q$ tomography. Attenuation tomography has the potential to better map out regional variability and to provide better path corrections. An advantage of the method presented here is that all the regional phases use the same coda-derived source spectra, so that any differences between phases in apparent $Q$ are due to true propagation differences between the different wave types. After applying the methodology to a region, the derived Q can be applied to direct waves of future events to determine source spectra. Inherent in this method is the fact that the direct wave and coda-derived source spectra will agree to within their natural variability. This can be useful for applications where spectra are used to derive source parameters of interest (e.g., moment, energy, earthquake-explosion discriminants) and consistency is desired between coda and direct results. Finally we have applied the method here to the standard four regional phases, but the same

methodology could be applied to other phases, including teleseismic P and S waves. Uncertainty in teleseismic attenuation is a factor in discrepancies between regional and teleseismic estimates of seismic parameters like energy (e.g. Perez-Campos, 2003) and application of this technique could help resolve the issue.

Apparent attenuation remains a very important parameter in local and regional seismology with applications that include predicting strong ground motion, studying earthquake source physics, and identifying explosions. The new technique presented here takes advantage of known source spectra from coda (or other means if available) to determine apparent $Q$ of direct regional phases. Future work will compare this new technique to other apparent attenuation methodologies that use different assumptions.

**Figures**

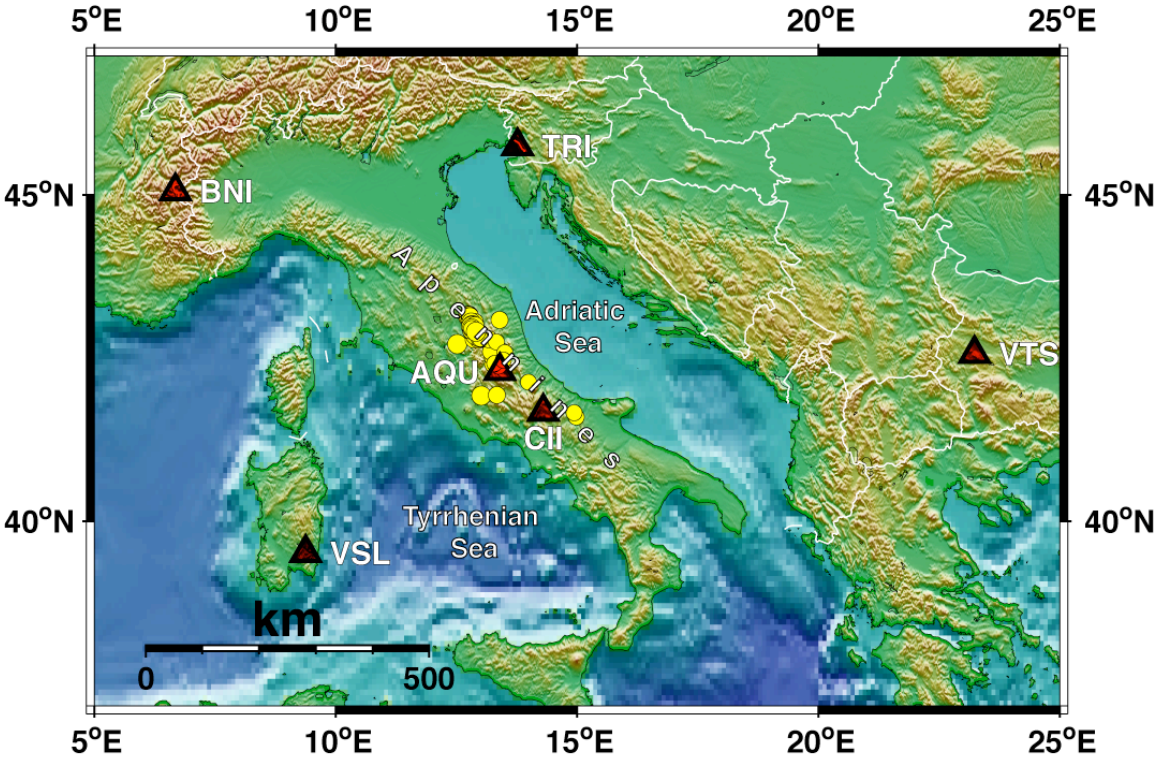


**Figure 1**. Shaded topography and bathymetry map of events (yellow circles) and stations (red triangles) used in this paper, with some geographic features labeled.

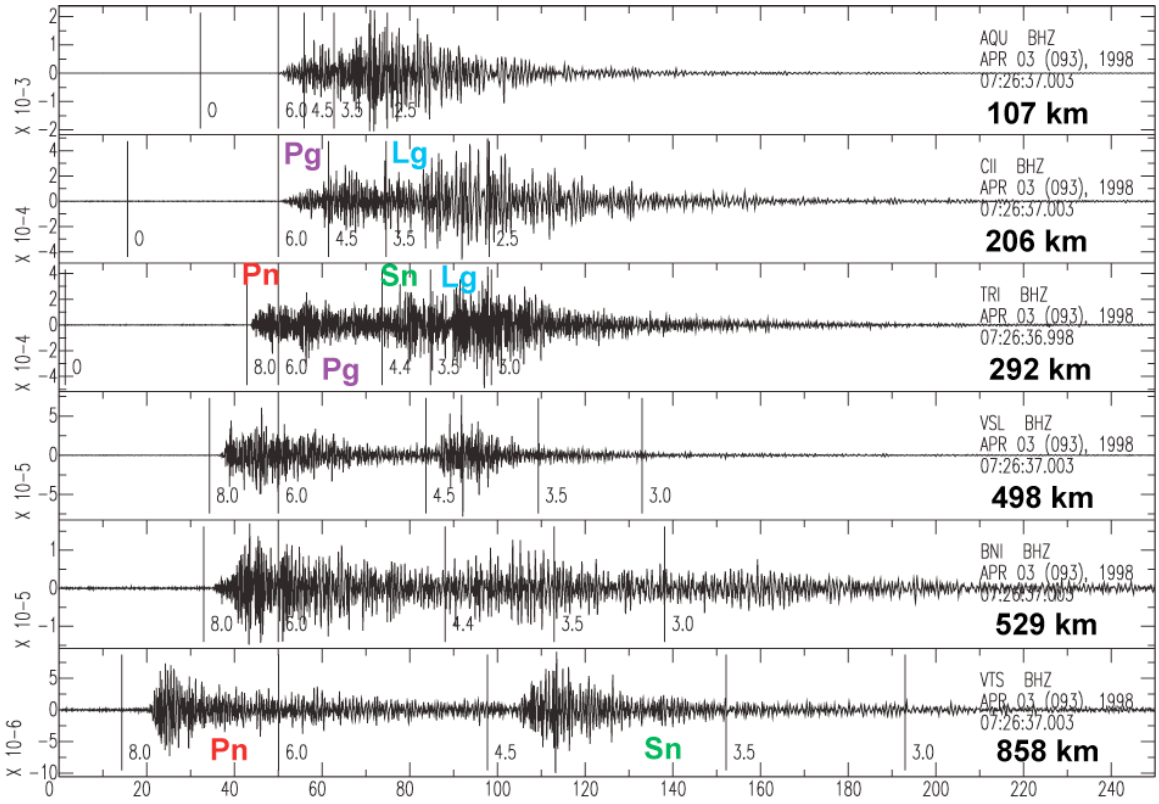


**Figure 2**. Example vertical component seismograms from an April 3, 1998 Mw 5 central Italian earthquake recorded at MEDNET stations. Traces are plotted at reduced velocity of 6 km/s and group velocity windows used to define phases are shown. Traces are instrument corrected to acceleration and bandpass filtered from 0.5 to 8 Hz.

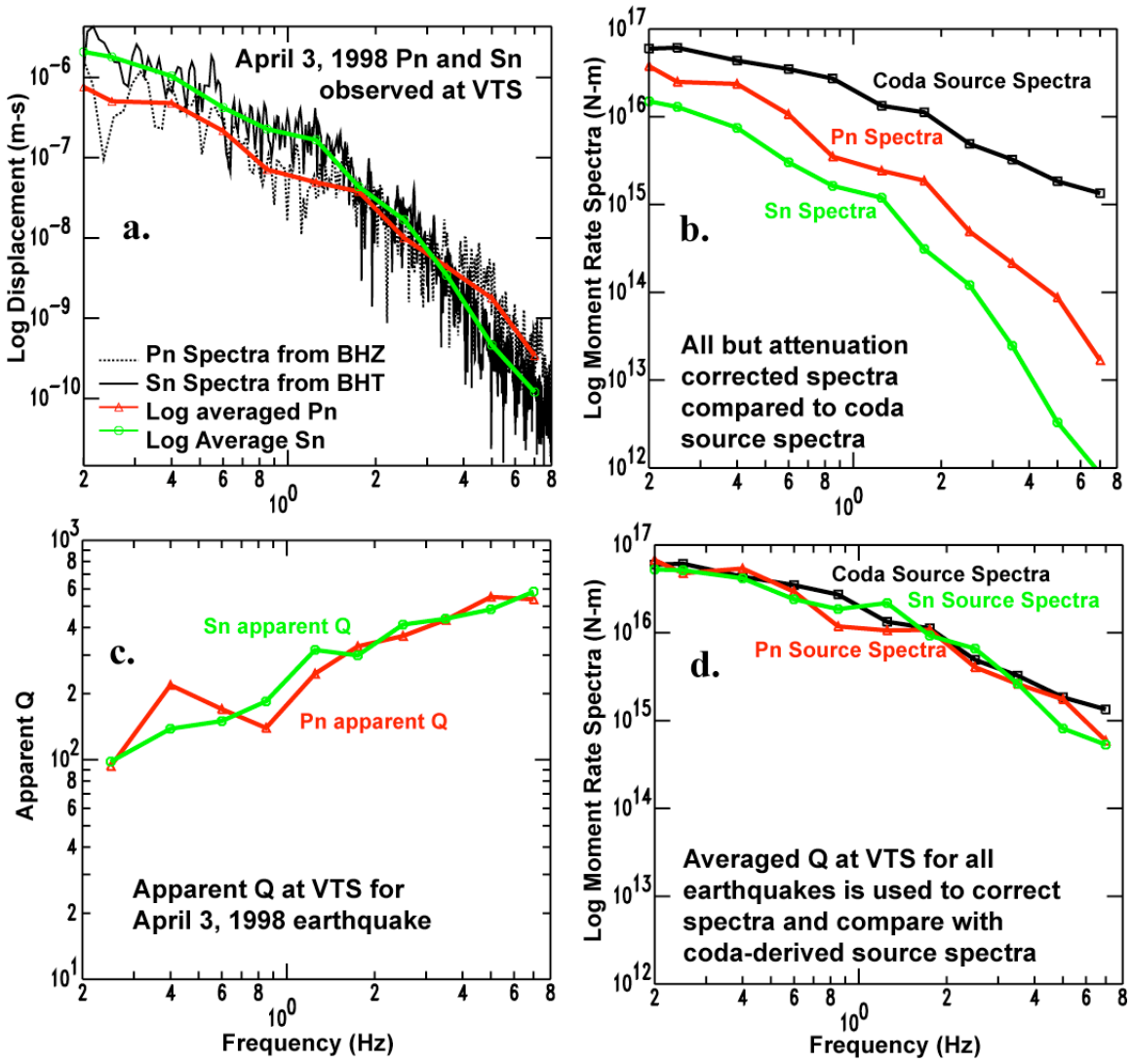


**Figure 3.** An illustration of the methodology using an event at station VTS. a) Instrument corrected displacement spectra for each of the regional phases is log averaged in the 11 bands where coda spectra were determined. b) The regional phase spectra are corrected for geometrical spreading and *F*-term and compared with the coda derived source spectra. The difference between the coda and the regional phase spectra is the apparent attenuation. c) The apparent $Q$ determined using equation 5 for this one earthquake at VTS. d) Using the VTS apparent $Q$ determined from all earthquakes (c.f. Table 1) the regional spectra are corrected to source spectra and compared with the coda –derived result. The small differences are due to the inherent scatter in the direct phases. See text for more detail.

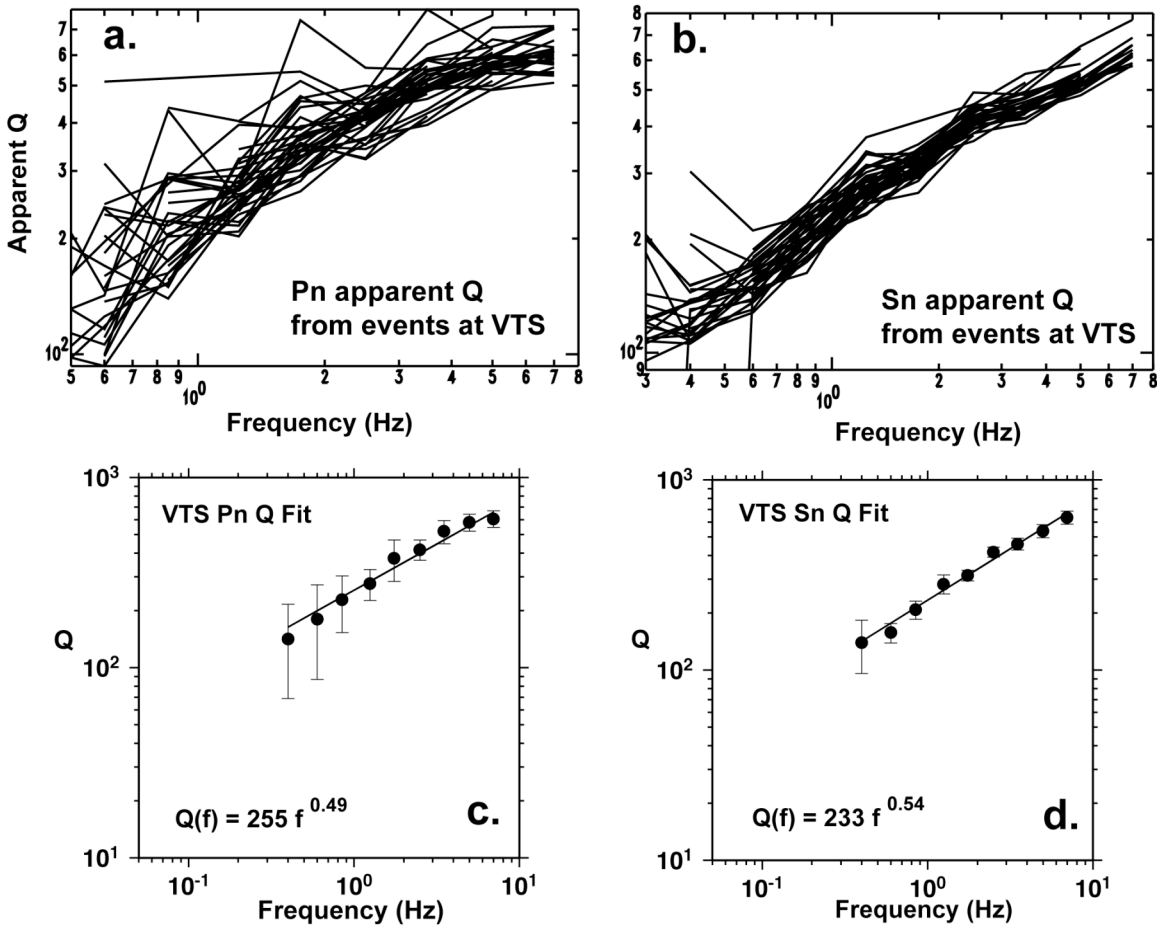


**Figure 4**. Example of Pn and Sn apparent *Q* results at station VTS for all events. In the top plots each event is shown as a separate line. In the bottom plots the log averaged *Q* values are shown with two sigma error bars and a best straight line (power law) fit.

**Table 1**
*Q*(*f*) Results with uncertainties for regional phases at 6 stations

| Station (distances) | Pn | Pg | Sn | Lg |
|---|---|---|---|---|
| AQU (53-153 km) | - | $45\pm23\ f^{0.45\pm0.25}$ $1.0 < f < 8.0$ | - | $78\pm26\ f^{0.40\pm0.18}$ $1.0 < f < 8.0$ |
| CII (53-206 km) | - | $61\pm18\ f^{0.48\pm0.17}$ $0.7 < f < 8$ Hz | - | $109\pm15 f^{0.27\pm0.10}$ $0.5 < f < 8$ Hz |
| TRI (291-352 km) | $121\pm28\ f^{0.83\pm0.17}$ $0.5 < f < 8$ Hz | $105\pm11\ f^{0.74\pm0.08}$ $0.5 < f < 8$ Hz | $132\pm15\ f^{0.76\pm0.09}$ $0.3 < f < 8$ Hz | $111\pm7\ f^{0.72\pm0.05}$ $0.2 < f < 8$ Hz |
| BNI (529-616 km) | $153\pm22\ f^{0.41\pm0.07}$ $0.5 < f < 8$ Hz | $96\pm4\ f^{0.61\pm0.04}$ $0.3 < f < 8$ Hz | $137\pm7\ f^{0.55\pm0.04}$ $0.5 < f < 8$ Hz | $102\pm3\ f^{0.68\pm0.03}$ $0.5 < f < 6$ Hz |
| VSL (412-526 km) | $244\pm83\ f^{0.69\pm0.24}$ $0.5 < f < 8$ Hz | - | $178\pm29\ f^{0.69\pm0.12}$ $0.5 < f < 8$ Hz | - |
| VTS (811-877 km) | $255\pm28\ f^{0.49\pm0.07}$ $0.3 < f < 8$ Hz | - | $233\pm11\ f^{0.54\pm0.04}$ $0.3 < f < 8$ Hz | - |
| Geometrical spreading exponent | 1.1 | 0.5 | 1.1 | 0.5 |

**Acknowledgements.** This work was begun during a two-week visit by W.W. and K.M. to INGV in October 2005 and we thank INGV for hosting us. This research was performed under the auspices of the U.S. Department of Energy by the University of California Lawrence Livermore National Laboratory under contract number W-7405-ENG-48. This research has been partially supported by the Dipartimento della Protezione Civile, under contract S4, ProCiv-INGV (2004-06), project: "Stima dello scuotimento in tempo reale e quasi-reale per terremoti significativi in territorio nazionale"

References:

Aki, K. and P. G. Richards, (1980). *Quantitative Seismology*, W. H. Freeman, New York.

Battone, S., M. D. Fisk and G. D. McCarter (2002), Regional Seismic-Event Characterization Using a Bayesian Formulation of Simple Kriging, *Bull. Seism. Soc. Am.*, *92*, p. 2277-2296.

Bindi, D., R. R. Castro, G. Franceschina, L. Luzi, and F. Pacor, The 1997-1998 Umbria-Marche sequence (central Italy): source, path and site effects estimated from strong motion data recorded in the epicentral area, *J. Geophys. Res.* Doi:10.1029/2003JB002857, 2004.

Doglioni, C., F. Mongelli, P. Pieri, 1994. The Puglia uplift (SE-Italy): an anomaly in the foreland of the Apenninic subduction due to the buckling of a thick continental litosphere. *Tectonics* 13, 1309-1321.

Eken, T., K. Mayeda, A. Hofstetter, R. Gök, G. Örgülü and N. Turkelli (2004), An application of the coda methodology for moment-rate spectra using broadband stations in Turkey, *Geophys. Res. Lett.* 31, 11, L11609.

Ekstrom, G., A. Morelli, E. Boschi and A. Dziewonski, Moment tensor analysis of the central Italy earthquake sequence of September-October 1997, *Geophys. Res. Lett. 25*, 1971-1974, 1998.

Galadini, F., and P. Galli, 2000. Active tectonics in the central Apennines (Italy) – Input data for Seismic Hazard Assessment. *Natural Hazard 22*, 225-270.

Malagnini, L., Akinci, A., Herrmann, R. B., Pino, N.A., Scognamiglio, L, 2002. Characteristics of the ground motion in Northeastern Italy, Bull. Seism. Soc. Am., 92, 2186-2204.

Malagnini, L., Herrmann, R.B., and M. Di Bona (2000). Ground motion scaling in the Apennines (Italy). Bull. Seism. Soc. Am.,90, 1062-1081.

Malagnini, L., and R.B., Herrmann (2000). Ground motion scaling in the region of the Umbria-Marche earthquake of 1997. Bull. Seism. Soc. Am., 90, 1041-1051.

Morasca, P., Malagnini, L., Akinci, A., Spallarossa D. (2006). Ground Motion Scaling in the Western Alps. *Journal of Seismology* (in press).

Malinverno, A., W. B. F. Ryan, 1986. Extension in the Tyrrhenian Sea and shortening in the Apennines as result of arc migration driven by sinking of the lithosphere. *Tectonics 5*, 227-245.

Mayeda, K., $m_b$ ($L_g$ coda): A stable single station estimator of magnitude. *Bull. Seismol. Soc. Am., 83*, 851-861, 1993.

Mayeda, K. M. and W. R. Walter, (1996). Moment, energy, stress drop and source spectra of Western U.S. earthquakes from regional coda envelopes, *J. Geophys. Res*., *101*, 11,195-11,208.

Mayeda, K., A. Hofstetter, J. L. O'Boyle, and W. R. Walter, (2003). Stable and transportable regional magnitudes based on coda-derived moment-rate spectra, *Bull. Seis. Soc. Am*., 93, 224-239.

Mayeda, K., R. Gök, W.R. Walter, A. Hofstetter, Evidence for non-constant energy/moment scaling from coda-derived source spectra, *Geophys. Res. Lett.* Doi:10.1029/2005GL022405, 2005.

Mele, Giuliana, Antonio Rovelli, Dogan Seber, and Muawia Barazangi, Mapping shear wave attenuation in the lithosphere beneath Italy and surrounding regions: Tectonic implications*, J. Geophys. Res., 102*, 11863-11875, 1997.

Montone, P., A. Amato, S. Pondrelli, 1999. Active stress map of Italy. *J. Geophys. Res. 104*, 25595-25610.

Morasca, P., K. Mayeda, L. Malagnini, and W.R. Walter (2005), Coda-derived source spectra, moment magnitudes, and energy-moment scaling in the western Alps, *Geophys. J. Int.* 160, 263-275.

Pantosti, D., G. D'Addezio, F. R. Cinti, 1996. Paleoseismicity of the Ovindoli-Pezza fault, central Apennines, Italy: a history including a large previously unrecorded earthquake in middle age. *J. Geophys. Res. 101*, 5937-5959.

Patacca, E., R. Sartori, P. Scandone, 1990. Tyrrenian basin and Apenninic arcs: kinematic relations since late Tortonian times. *Mem. Soc. Geol. Ital. 45*, 425-451.

Perez-Campos, X., S. K. Singh, and G. C. Beroza, (2003). Reconciling teleseismic and regional estimates of seismic energy, *Bull. Seism. Soc. Am., 93*, 2123-2130.

Pondrelli, S., S. Salimbeni, G. Ekström, A. Morelli, P. Gasperini and G. Vannucci, The Italian CMT dataset from 1977 to the present, *Phys. Earth Planet. Int., doi:10.1016/j.pepi.2006.07.008,159*, 286-303, 2006.

Royden, L., E. Patacca, P. Scandone, 1987. Segmentation and configuration of subducted lithosphere in Italy: an important control on thrust-belt and foredeep-basin evolution. *Geology 15* (7), 14-717.

Sereno, T.J. and J.W. Given (1990). Pn attenuation for a spherically symmetric earth model, *Geophys. Res. Lett.,* 17, 1141-1144.

Street, R. L., R. Herrmann, and O. Nuttli (1975). Spectral characteristics of the Lg wave generated by central United States earthquakes*, Geophys. J. R. Astron. Soc*. **41**, 51-63.

Taylor, S., A. Velasco, H. Hartse, W. S. Philips, W. R. Walter, and A. Rodgers, (2002). Amplitude corrections for regional discrimination, *Pure. App. Geophys*. *159*, 623-650.